Monthly Notices of the ROYAL ASTRONOMICAL SOCIETY

MNRAS **529,** 1130–1137 (2024) https://doi.org/10.1093/mnras/stae403
Advance Access publication 2024 February 7

The rise and fall of dust in the Universe

Stephen Eales★ and Bradley Ward
Cardiff Hub for Astrophysics Research and Technology, School of Physics and Astronomy, Queen's Buildings, 5 The Parade, Cardiff CF24 3AA, UK

Accepted 2024 January 31. Received 2024 January 30; in original form 2023 October 18

ABSTRACT

We estimate how the mean density of dust in the Universe varies with redshift, using submillimetre continuum observations and a method designed to minimize the effect of dust temperature. We have used the *Herschel* Astrophysical Terahertz Large Area Survey (*Herschel*-ATLAS) to show that the median temperature of dust in galaxies is $\simeq 22$ K and does not vary significantly with redshift out to $z = 1$. With this as our estimate of the mass-weighted dust temperature, we have used an 850-μm survey of the field of the Cosmological Evolution Survey (COSMOS) to estimate the mean density of dust in 10 redshift bins over the range $0 < z < 5.5$. We find that the mean density of dust increased by a factor of $\simeq$10 from $z = 5$ to $z = 2$, declined slightly to $z = 1$, and then steeply to the present day. The relationship between the mean density of dust and redshift is similar to the relationship between the mean star formation rate and redshift, although the increase for the former is steeper from $z = 5$ to $z = 2$. We have also used the submillimetre measurements to estimate the mean density of gas over the same redshift range. The values we estimate for the dust-traced gas are much lower and with a different redshift dependence than those for estimates of the mean density of atomic gas but similar to those for estimates of the mean density of the CO-traced gas. We find that the depletion time for the dust-traced gas in the Universe as a whole declines with redshift in the same way as seen for individual galaxies.

Key words: galaxies: evolution – galaxies: ISM – submillimetre: galaxies.

1 INTRODUCTION

Dust is one of the most important substances in the Universe, being the critical coolant in star formation regions and being responsible for the formation of molecular hydrogen, which in turn makes it indirectly responsible for the creation of stars and planets. Apart from these important astrophysical roles and its intellectual interest, dust is also a valuable astronomical tool as a tracer of the interstellar medium (ISM). CO, the traditional tracer of the molecular phase for the last 50 yr, has many well-known problems, and the use of the continuum emission from dust as an alternative method of tracing the molecular phase of the ISM (Eales et al. 2012; Scoville et al. 2014) has many advantages: dust grains are more robust than CO molecules; it is much easier to detect the dust in galaxies than the CO ($\sim 10^6$ detections of galaxies in the *Herschel* archive); and, if the metal abundance in the galaxy is known, the relationship between the dust-to-gas ratio and metal abundance is much simpler than the relationship between the CO *X*-factor and metal abundance (Bolatto, Wolfire & Leroy 2013; Rémy-Ruyer et al. 2014). Observations of the dust in large samples of galaxies are already giving valuable insights into galaxy evolution. For example, the rapid low-redshift evolution seen in the submillimetre luminosity function (Dye et al. 2010) and the dust-mass function (Dunne et al. 2011) is not reproduced by cosmological simulations (Eales et al. 2018; Millard et al. 2021).

In this paper, we do not consider the dust content of individual galaxies, but we instead describe an attempt to determine how the mean density of dust depends on redshift. There are three main methods that have been used to derive this relationship: (i) from the absorption-line systems in quasars, for which the line ratios can be used to estimate both the metal abundance and the fraction of metals locked up in the dust; (ii) from the dust reddening of the quasars with absorption-line systems; and (iii) from the continuum emission of the dust in galaxies (Péroux & Howk 2020). The main disadvantage of the first two methods is that the dust in the absorption-line system reduces the optical brightness of the quasar, creating a selection bias against quasars behind dust-rich absorption-line systems being included in quasar catalogues (Péroux & Howk 2020).

In this paper, we apply the third of the methods. This does not suffer from the potential selection bias of the other two but has problems of its own. The method relies on the assumption that the constant of proportionality between the dust mass and the submillimetre luminosity is independent of redshift. We cannot be completely confident of this assumption, although there is evidence that the dust emissivity index, which is dependent on the structures and chemistry of the dust grains, does not change with redshift (Ismail et al. 2023; Witstok et al. 2023; Ward et al., submitted). This, however, is only a potential problem. An actual problem is that the emission from the dust also depends on the temperature of the dust.

Something that limits the accuracy of all attempts to measure the temperature of the dust in galaxies is that warm dust emits more radiation than the same mass of cold dust. This means that the temperature estimated from the best-fitting spectral energy

★ E-mail: EalesSA@Cardiff.ac.uk

distribution (SED), the luminosity-weighted mean dust temperature, will always be higher than the more meaningful mass-weighted mean dust temperature unless the temperature of the dust is everywhere the same in the galaxy (Eales, Wynn-Williams & Duncan 1989). The effect of this bias on the estimate of the dust mass depends on the rest-frame wavelength of the flux density used to estimate the dust mass. The effect is less for wavelengths on the long-wavelength (Rayleigh–Jeans) side of the peak in the dust SED, since at infinite wavelength the continuum emission depends on only the first power of dust temperature. The effect of the temperature bias can therefore be reduced by estimating the dust masses from a survey carried out at as long a wavelength as possible. This is the approach we have followed in this paper, in which the dust masses have been estimated from a survey at 850 μm.

This paper is arranged as follows. In Section 2, we describe the method. Section 3 gives the results. We discuss the results in Section 4 and list our conclusions in Section 5. We use the cosmological parameters given in Planck Collaboration XXII (2015).

2 METHODS

2.1 The temperature of the dust

The SED of the dust in a typical galaxy has a peak in the rest frame at $\lambda_{\rm peak} \simeq 100$ μm. If a small amount of hot dust is added to the galaxy, it will have most effect on the SED at wavelengths $< \lambda_{\rm peak}$. One might therefore hope to get a more accurate estimate of the mass-weighted dust temperature from fitting a modified blackbody to the galaxy's flux measurements if the fit only uses flux measurements at $\lambda > \lambda_{\rm peak}$. Empirically, this seems to be true. Estimates of dust temperature for galaxy samples in which flux measurements at shorter wavelengths are included (e.g. Dunne et al. 2000; Vlahakis, Dunne & Eales 2005) are much higher than ones in which only flux measurements at longer wavelengths are included (e.g. Eales et al. 2012; Cortese et al. 2014). There is also evidence for individual galaxies that inclusion of a flux measurement at a wavelength shorter than the peak increases the estimate of the dust temperature (Smith et al. 2010, 2012).

With this in mind, we have estimated dust temperatures from the galaxies discovered in the *Herschel*-ATLAS (H-ATLAS), a survey of 660 deg^2 carried out with the *Herschel Space Observatory* (Eales et al. 2010; Bourne et al. 2016; Valiante et al. 2016; Smith et al. 2017; Furlanetto et al. 2018; Maddox et al. 2018; Ward et al. 2022) at 100, 160, 250, 350, and 500 μm. The advantages of this survey are that it provides long-wavelength photometry for a very large number of galaxies. The H-ATLAS photometry is most sensitive at the three longest wavelengths and in the rest frame these wavelengths are $> \lambda_{\rm peak}$ at the highest redshifts we consider.

We used the catalogue of sources from the H-ATLAS field at the south galactic pole, which covers 317.6 deg^2 (Maddox et al. 2018; Ward et al. 2022). We used the subset of 81 895 sources for which there is both a probable counterpart and a redshift (Ward et al. 2022). The redshifts are photometric redshifts estimated from the available multiwavelength images for this field (Ward et al. 2022). Each of the sources in this sample was detected at $>4\sigma$ at at least one of the following wavelengths: 250, 350, and 500 μm. Each source has a flux measurement at all five H-ATLAS wavelengths.

We fitted the standard modified blackbody equation to the five flux densities available for each source:

$$F_\nu \propto B(\nu)\nu^\beta, \quad (1)$$

in which β is the dust emissivity index. We used a value of β of 2, which is typical of the values found in most recent studies of high-redshift galaxies (Bendo et al. 2023; Ismail et al. 2023; Witstok et al. 2023; Ward et al., submitted).

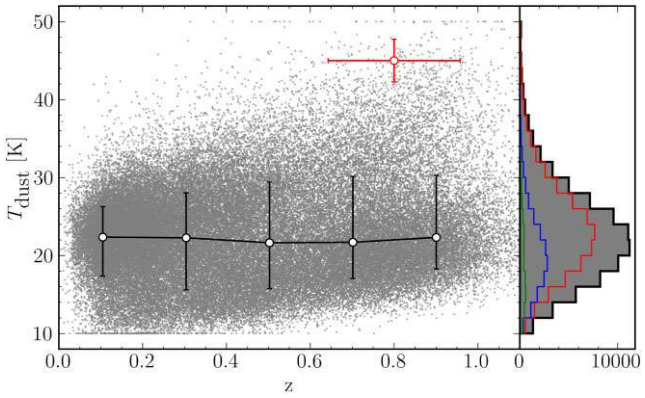

Figure 1. Plot of dust temperature against redshift for 81 895 galaxies in the SGP field of the H-ATLAS. The red cross shows the typical $\pm1\sigma$ uncertainty in the photometric redshift and temperature estimate. The open circles show the median dust temperatures in five redshift bins, each of width 0.2, with the error bar showing 16th to 84th percentiles of the temperature distribution. The panel to the right shows the histogram of dust temperature for all galaxies (filled-in histogram), galaxies with S/N > 4 in one band (red), in two bands (blue), and in three bands (green).

Table 1. The median dust temperature.

Redshift	$T_{\rm d}$ (K)
$0.0 < z < 0.2$	$22.4^{+3.9}_{-5.0}$
$0.2 < z < 0.4$	$22.3^{+5.7}_{-6.7}$
$0.4 < z < 0.6$	$21.7^{+7.7}_{-5.9}$
$0.6 < z < 0.8$	$21.7^{+8.5}_{-4.7}$
$0.8 < z < 1.0$	$22.3^{+8.0}_{-4.1}$

Fig. 1 shows the median dust temperature of the sources in five redshift bins. Table 1 lists the median values and the 16th to 84th percentiles of the temperature distribution in each bin. Over the redshift range $0 < z < 1$, there is no evidence of any evolution in dust temperature. The median dust temperature in all bins is $\simeq$22 K. The right-hand panel in the figure shows the histograms of dust temperature for sources for which there are detections at $>4\sigma$ at one, two, or three of the *Herschel* wavelengths. The panel shows that the median dust temperature would be lower if we only considered sources with at least two or three significant detections. However, this might be a selection effect because it is more likely that there will be an additional significant detection at $\lambda > 250$ μm if the galaxy is colder. We therefore decided to use the median dust temperature derived from the entire sample.

There is no consensus in the literature about whether dust temperature increases with redshift at $z > 1$, with some studies finding positive evolution (Magnelli et al. 2014; Béthermin et al. 2015; Schreiber et al. 2018; Zavala et al. 2018; Drew & Casey 2022) and others no evolution (Dudzevičiūtė et al. 2020; Lim et al. 2020; Barger et al. 2022). A fundamental limitation of these studies is that they all measure the luminosity-weighted rather than the mass-weighted dust temperature. We have recently estimated the dust temperature in a sample of 100 dusty star-forming galaxies in the redshift range $2 < z < 6$ (Ward et al., submitted), in which we have used only photometry

on the long-wavelength side of the dust peak (see above). We found no evolution in the temperature of the dust over this redshift range.

Models that use simulations of galaxies over the redshift range $2 < z < 6$ from the *Feedback in Realistic Environments* (FIRE) project show (a) that the luminosity-weighted dust temperature ($T_{\rm eff}$ in their nomenclature) is often $\simeq$10 K higher than the mass-weighted dust temperature and (b) that the mass-weighted dust temperature does not evolve strongly with redshift (Liang et al. 2019). 68 per cent of the simulated galaxies in this study have mass-weighted dust temperatures in the range $T_{\rm d} = 25 \pm 5$ K, which is not too far off the values we measure at $z < 1$.

Given the results of the FIRE simulations and the lack of any clear contrary observational evidence, in the rest of this paper we have assumed that the median dust temperature at all redshifts is 22 K, although we have explored the consequences if this assumption is not correct.

2.2 Calculating the dust density

In our analysis, we have combined two sets of results for the COSMOS field. First, Davidzon et al. (2017) have measured the stellar mass function (SMF) in the field in 10 redshift slices over the redshift range $0 < z < 5.5$. Secondly, Millard et al. (2020) used a stacking analysis on the S2COSMOS 850-μm survey of the COSMOS field (Simpson et al. 2017) to measure the mean 850-μm flux of 64 684 galaxies, separated into bins of stellar mass and redshift, in the field. We have combined these two data sets to estimate the mean density of dust in each redshift bin.

We have calculated the dust mass from the flux density at 850 μm (Millard et al. 2020) using the equation:

$$M_{\rm d} = \frac{\langle S_{850\,\mu{\rm m}}\rangle D_{\rm L}^2}{(1+z)B(\nu_{\rm e})\kappa(\nu_{\rm e})}, \tag{2}$$

in which $\nu_{\rm e}$ is the frequency in the rest frame: $\nu_{\rm e} = (1+z)\nu_{850\,\mu{\rm m}}$. $D_{\rm L}$ is luminosity distance, $\langle S_{850\,\mu{\rm m}}\rangle$ is the mean flux density given by Millard et al. (2020), and the dust mass-opacity coefficient, $\kappa(\nu)$, is given by

$$\kappa(\nu) = \left(\frac{\nu}{\nu_{850\,\mu{\rm m}}}\right)^{\beta} \kappa_{850\,\mu{\rm m}}. \tag{3}$$

We assumed a value for β of 2 (see above), a value for the dust temperature of 22 K, and the widely used value for the mass-opacity coefficient of $\kappa_{850\,\mu{\rm m}} = 0.077$ m^2 kg^{-1} (James et al. 2002; da Cunha, Charlot & Elbaz 2008; Dunne et al. 2011). Before calculating the dust mass, we corrected the flux density and the dust temperature for the effect of the cosmic microwave background using the method in da Cunha et al. (2013) (equations 12 and 18 in that paper).

Fig. 2 shows the ratio of the mean value of the dust mass to the median stellar mass for each redshift bin plotted against stellar mass, using the mean redshift and median stellar mass for each bin (see table D1 of Millard et al. 2020). For each of the bins, we fitted the following relationship to the data points:

$$\frac{M_{\rm d}}{M_{\rm s}} = a \log_{10} M_{\rm s} + b. \tag{4}$$

Table 2 lists our estimates of a and b and the values of the weighted mean ratio of dust mass to stellar mass for each of the redshift bins. There is a clear relationship between the mass ratio and stellar mass for the five low-redshift bins, with the best-fitting relationship shown in the figure. For the other five bins, the dashed line in the figure shows the weighted mean value of the mass ratio.

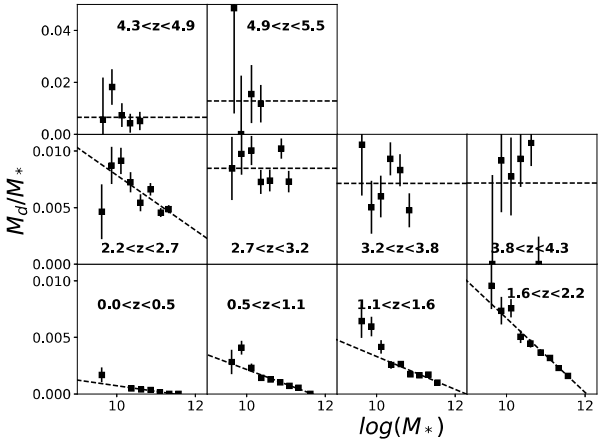

Figure 2. Plot of the ratio of dust mass to stellar mass against stellar mass for the redshift ranges used by Millard et al. (2020). For the five low-redshift bins, the dashed lines show the best-fitting linear relationships (equation 4; Table 2). For the five high-redshift bins, the dashed lines show the weighted mean value of the mass ratio (Table 2).

Table 2. Fits to $M_{\rm d}/M_{\rm s}$ versus $M_{\rm s}$ (Fig. 2).

Redshift	a	b	$\langle M_{\rm d}/M_* \rangle$
$0.0 < z < 0.5$	−0.00050	0.0057	0.00014 ± 0.00002
$0.5 < z < 1.1$	−0.00130	0.0152	0.00076 ± 0.00004
$1.1 < z < 1.6$	−0.00146	0.0179	0.0018 ± 0.00006
$1.6 < z < 2.2$	−0.00329	0.0396	0.0031 ± 0.0001
$2.2 < z < 2.7$	−0.00244	0.0323	0.0054 ± 0.0002
$2.7 < z < 3.2$	−0.00058	0.0146	0.0085 ± 0.0004
$3.2 < z < 3.8$	−0.00105	0.0181	0.0071 ± 0.0007
$3.8 < z < 4.3$	−0.00459	0.0553	0.0072 ± 0.0012
$4.3 < z < 4.9$	−0.01115	0.1217	0.0065 ± 0.0021
$4.9 < z < 5.5$	−0.00866	0.1015	0.0128 ± 0.0058

We calculated the mean density of dust, ρ_i, in the ith bin of stellar mass and redshift from the equation:

$$\rho_i = \frac{\int_{z_{\rm L}}^{z_{\rm U}} \int_{M_{\rm L}}^{M_{\rm U}} \phi(M_{\rm s}) M_{\rm d}(z) {\rm d}M_{\rm s} {\rm d}V}{\int_{z_L}^{z_{\rm U}} {\rm d}V} \tag{5}$$

in which $M_{\rm s}$ is the mass of stars in a galaxy and the dust mass is calculated from the mean flux density given in Millard et al. (2020) using equation (2). We did not interpolate across a bin using the relationships given in Table 2 because this is not consistent with the stacking method used in the earlier paper.

The mean density of dust in each redshift bin is then given by

$$\rho = \sum_i \rho_i + c, \tag{6}$$

in which the sum is over all the stellar mass bins for that redshift slice and c is a correction factor to include the contribution to the dust density from galaxies outside the range covered by the stacking analysis (Millard et al. 2020). We chose to estimate the mean density of dust for galaxies with a stellar mass in the range $9.0 < \log_{10}(M_*) < 11.75$ and calculated c using the stellar mass function and the relationships shown in Fig. 2. For the five low-redshift bins, we used the best-fitting linear relationship. For the five high-redshift bins, for which there is not a clear trend between the mass ratio and stellar mass, we used the weighted mean value of the mass ratio to calculate c, but we also made an estimate of c using the best-fitting linear relationship. We used the difference between the two estimates of c

Table 3. The mean density of dust.

Redshift	$\langle z \rangle$	$\langle \rho_{\rm dust} \rangle$ (10^5 M$_\odot$ Mpc^{-3})	Correction[a] (10^5 M$_\odot$ Mpc^{-3})
$0.0 < z < 0.5$	0.28	0.85 ± 0.11	0.10
$0.5 < z < 1.1$	0.82	2.27 ± 0.13	0.22
$1.1 < z < 1.6$	1.36	2.69 ± 0.12	0.20
$1.6 < z < 2.2$	1.90	2.96 ± 0.12	0.34
$2.2 < z < 2.7$	2.44	2.09 ± 0.12	0.32
$2.7 < z < 3.2$	2.98	1.68 ± 0.11	0.30
$3.2 < z < 3.8$	3.52	0.78 ± 0.11	0.22
$3.8 < z < 4.3$	4.05	0.54 ± 0.14	0.19
$4.3 < z < 4.9$	4.59	0.40 ± 0.24	0.15
$4.9 < z < 5.5$	5.13	0.67 ± 0.41	0.26

[a]The correction has been included in the estimate in column 3.

as a systematic error, which we added in quadrature to the regular error. The contribution of c (Table 3) to the mean dust density only exceeds 20 per cent at $z > 3$. We calculated the statistical errors in the mean dust density by combining in quadrature the errors in the mean dust density in each stellar mass/redshift bin which arise from the error in the mean 850-μm flux density for that bin.

3 RESULTS

Fig. 3 shows our estimates of the mean density of dust in each redshift bin, with values listed in Table 3. To assess the possible systematic errors caused by errors in our assumption about dust temperature, we also estimated the mean density of dust using dust temperatures of 30, 25, 20, and 15 K. The estimates for each temperature are linked by the grey lines in the figure. The grey lines show that the main consequence if our assumption about the mean temperature of dust is incorrect is a change in the overall amplitude of the relationship between mean dust density and redshift rather than its shape, which is a result of the long wavelength used in the stacking analysis (on the Rayleigh–Jeans tail of a modified blackbody, emission is proportional to dust temperature). These lines also make it clear what would happen if our assumption that the mass-weighted temperature of dust is independent of redshift is incorrect. If, as some have claimed (Section 2.2), dust temperature increases with redshift, the decline in the mean density of dust at $z > 2$ would be steeper than we have estimated.

Our analysis shows that the mean density of dust in the Universe increased by a factor of $\simeq$10 from $z = 5$ to $z = 2$. There is then marginal evidence (1.6σ) for a decline from the bin for $1.6 < z < 2.2$ to the bin for $1.1 < z < 1.6$. The mean dust density then declined steeply to the present day. We have also plotted in the figure some previous estimates of the mean dust density. The previous estimates, considered as a whole, agree with our results, but there are interesting discrepancies between the different data sets.

The estimates that are most comparable to ours are those of Dunne et al. (2011) and Pozzi et al. (2020), who also used the submillimetre emission from dust to estimate the mean density of dust. The three data sets agree well about the rapid increase at $z < 1$, but our estimates are systematically lower than the other two. The obvious explanation of the difference in the one case is that Pozzi et al. (2020) used a value for the mass-opacity coefficient a factor of $\simeq$2 lower than we did, which will increase their estimates relative to ours by the same factor. Even with this correction, their values begin to diverge substantially from ours at $z > 1$, but at high redshifts their estimates are likely to be less reliable because their short selection wavelength (160 μm) means that their mass estimates will be highly dependent on dust temperature. The reason for the difference in the other case is less clear because if $\beta = 2$, we and Dunne et al. (2011) used the same values for the mass-opacity coefficient. However, because we used samples selected at different wavelengths (850 and 250 μm), a small difference in β would lead to a large change in the mass-opacity coefficient. If the mass-opacity coefficient is fixed at 850 μm, an increase in β of 0.3, for example, would increase the mass-opacity coefficient at 250 μm by $\simeq$44 per cent, which would decrease the mass estimates by the same factor.

The approach used by Driver et al. (2018) is a hybrid one in which all of their galaxies have submillimetre observations but most do not have significant submillimetre detections, with the dust masses being estimated from fits to the multiwavelength photometry (UV to submm) with the MAGPHYS modelling programme (da Cunha et al. 2008). They do not find the rapid low-redshift evolution in the mean density of dust seen by us and in the other two submillimetre papers.

Our estimates agree well at $z > 2.5$ and $z < 1$ with the estimates by Péroux & Howk (2020) from the line ratios in quasar absorption-line systems, but they are much higher than the absorption-line estimates in the intervening redshift range, which is the redshift range in which we find the mean dust density is at its peak. We speculate that the difference might be caused by the selection bias from dust in the absorption line systems (Section 1) being greatest in this redshift range. Our estimates do not agree well with the estimates from the reddening of quasar absorption-line systems (Ménard et al. 2010; Ménard & Fukugita 2012) at any redshift.

4 DISCUSSION

Fig. 4 shows our measurements of the mean density of dust plotted against redshift overplotted with a compilation of measurements of the mean star formation rate in the universe (Madau & Dickinson 2014). The line is a relationship that is a good fit to the measurements of the mean star formation rate (Madau & Dickinson 2014). We have chosen the offset between the mean star formation rate (shown on the right) and the mean dust density (shown on the left) so that the two sets of measurements roughly coincide. Although the vertical positioning is arbitrary, the figure shows that the redshift dependences of the two relationships are similar. Both the mean density of dust and the mean star formation rate peak at $z \sim 2$, and the two depend on redshift in similar ways except that the decline with redshift at $z > 2$ is steeper for the dust than for the star formation rate.

We have also used our results to estimate how the mean density of gas in the Universe varies with redshift (Section 1). To estimate this, it is not necessary to know the values of the dust mass-opacity coefficient or the gas-to-dust ratio. Instead, in a similar way to the other ISM tracers, CO molecules and carbon atoms (Dunne et al. 2022), the mass of the molecular ISM can be estimated directly from the submillimetre luminosity:

$$M_{\rm H_2} = \alpha_{\rm submm} L_{\rm submm} \quad (7)$$

as long as the constant of proportionality in the equation is known. There are several estimates of $\alpha_{\rm submm}$ in the literature (Scoville et al. 2014; Tacconi, Genzel & Sternberg 2020; Dunne et al. 2022), all of which are fairly consistent. We have used the value in Dunne et al. (2022) because these authors used a method that produced mutually consistent estimates of the values of α for the three standard tracers: CO, atomic carbon (CI), and dust. We used a value of $\alpha_{850\,\mu\rm m} = 1.066 \times 10^{-13}$ M$_\odot$ Hz W^{-1}, a factor of 1.36 lower than the value given in Dunne et al. (2022), in order that our mass estimates would not include the contribution of helium. Fig. 5 shows our results. The

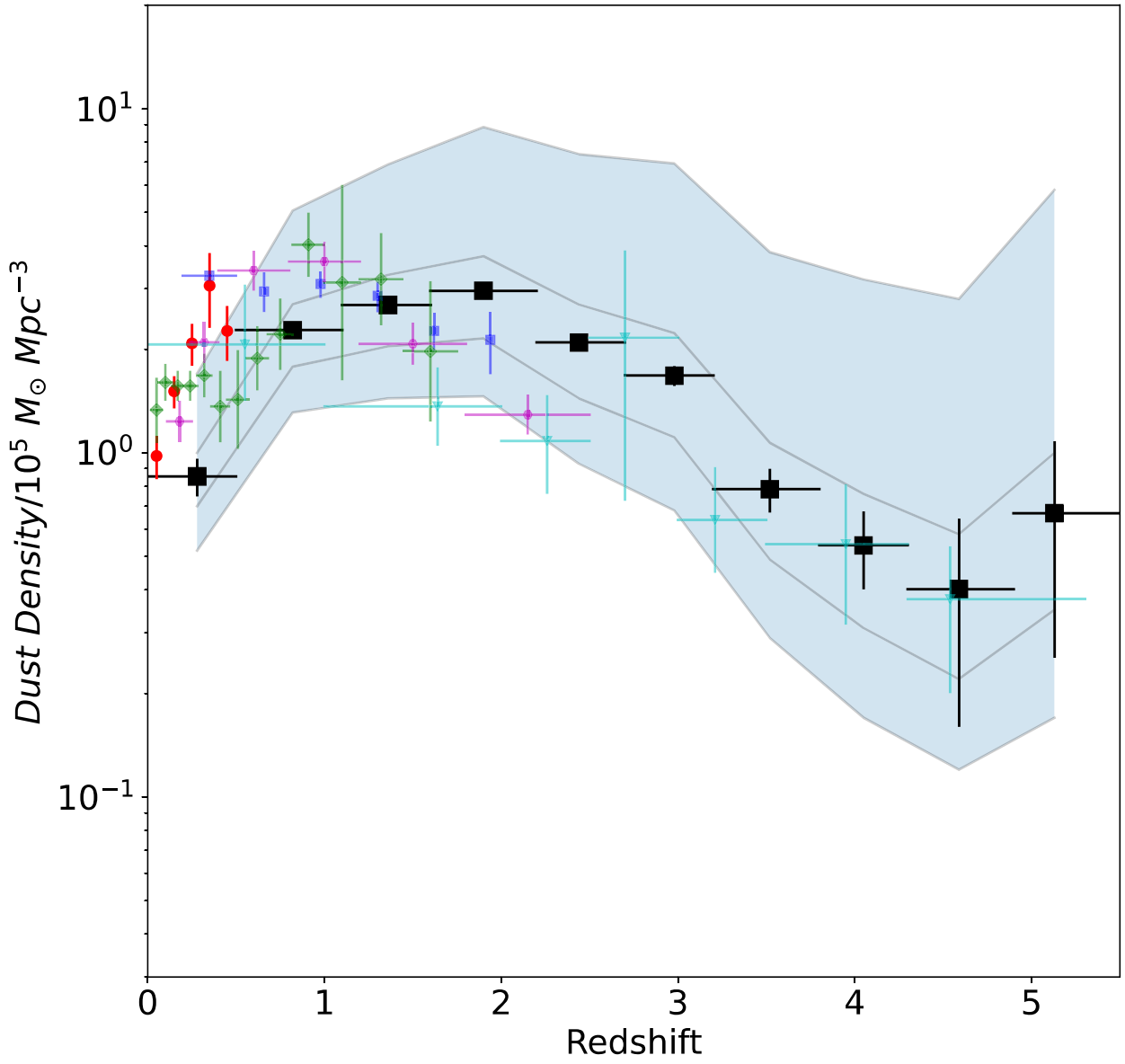

Figure 3. Mean density of dust in the Universe versus redshift. The large black squares are our estimates (Table 3). The four grey lines link our estimates if we repeat the analysis using dust temperatures, from bottom to top, of 30, 25, 20, and 15 K. The other symbols show previous estimates of the dust density: red (Dunne et al. 2011), blue (Ménard et al. 2010; Ménard & Fukugita 2012), green (Driver et al. 2018), mauve (Pozzi et al. 2020), and cyan (Péroux & Howk 2020). We have taken the values for all except the first from the useful compilation of Péroux & Howk (2020).

green symbols show the estimates from another recent study that also used the continuum emission from the dust to trace the gas (Garratt et al. 2021). This study found a similar rise and fall of the gas density with redshift that we see, although there are significant differences between our and their estimates at some redshifts.

The coloured lines and bands in the figure show the best current estimates, and their uncertainties, of the mean density of atomic hydrogen (red) and of molecular hydrogen (blue) (Péroux & Howk 2020). The molecular hydrogen estimates come from observations of another tracer, CO, and were originlly made with a value for α_{CO} of 3.6 $M_\odot$ (K km s^{-1} pc^2)$^{-1}$ (Walter et al. 2014; Decarli et al. 2016, 2019; Riechers et al. 2019). Although this is similar to the value found by Dunne et al. (2022), 4.0 $M_\odot$ (K km s^{-1} pc^2)$^{-1}$, the latter value includes helium while the other value does not. Since Dunne et al. (2022) obtained estimates of the values of α for the three tracers in a self-consistent way, we have scaled the CO measurements to a value for α_{CO} of 2.94 $M_\odot$ (K km s^{-1} pc^2)$^{-1}$, which is the value given by Dunne et al. (2022) with the contribution of the helium removed.

There are large differences, in both redshift dependence and normalization, between our estimates and the relationship for atomic hydrogen. The similarity in the shapes between the relationships derived from the two tracers, CO and dust, implies that cosmic dust is mostly found in molecular gas.

The dust-traced gas points agree well with the CO-traced gas estimates at $z < 1$ but are significantly lower at higher redshift. One possible explanation is that our estimate of the mass-weighted dust temperature is still too high. The faint points in the figure show the effect of using a dust temperature of 18 K rather than 22 K, which is enough to make the estimates from the CO and dust consistent within

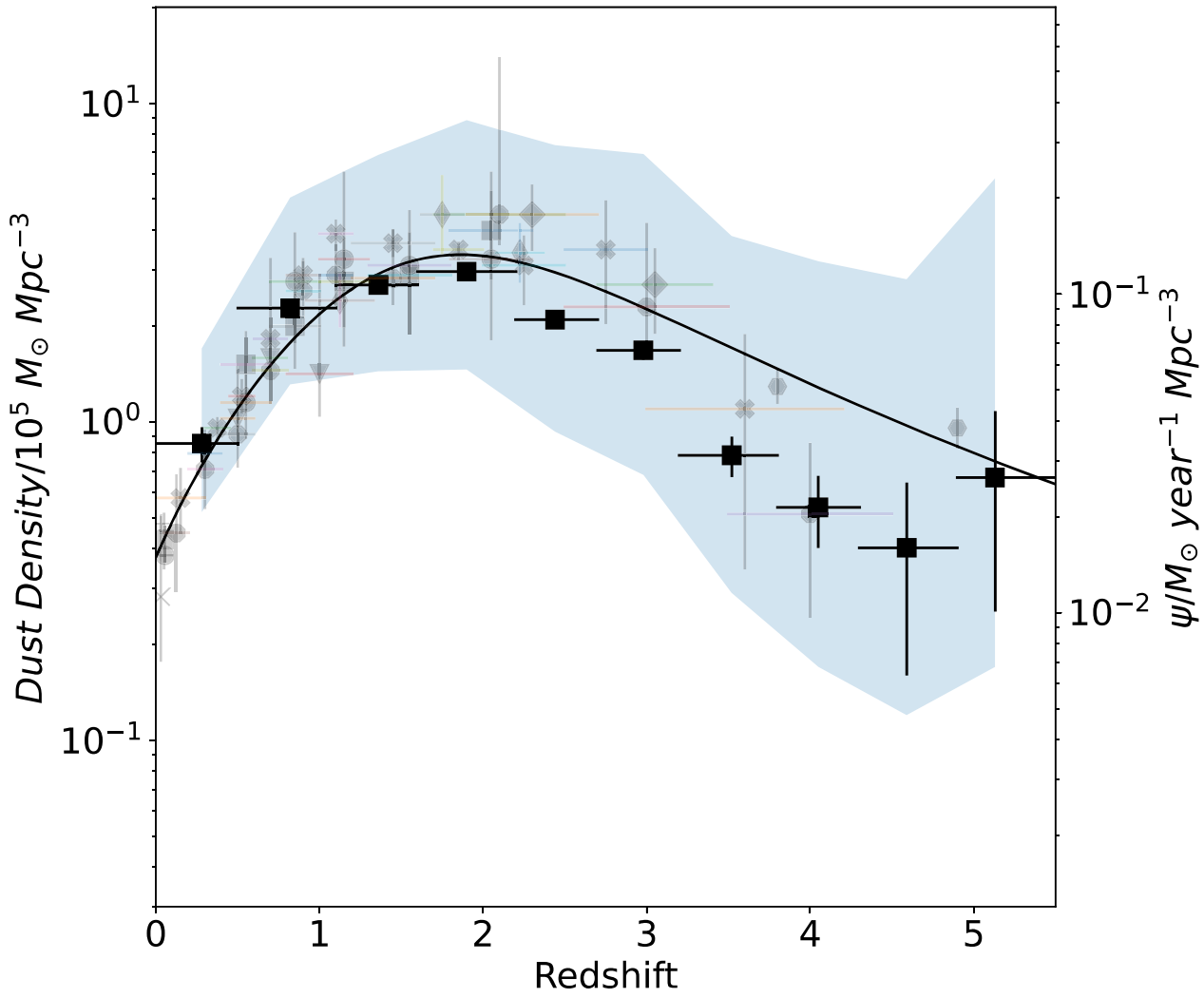

Figure 4. Mean density of dust versus redshift with overplotted estimates of the mean star formation rate in the Universe. The large black squares are our estimates of the mean density of dust (Table 3). The other symbols are estimates of the mean star formation rate in the Universe (Madau & Dickinson 2014), with the solid line showing a relationship that is a good fit to these measurements (Madau & Dickinson 2014). The vertical position of the star formation measurements has been chosen to roughly coincide with the dust measurements.

the errors. Another possible explanation is that the ratio $\alpha_{\rm CO}/\alpha_{\rm submm}$ depends on redshift, although Dunne et al. (2022) concluded that this ratio is roughly constant over the redshift range $0 < z < 6$.

The depletion time is the time needed for star formation to consume all the gas in a galaxy if no more is accreted. It is given by

$$\tau_{\rm dep} = \frac{M_{\rm gas}}{\rm SFR}. \quad (8)$$

It is possible to use the estimates of the mean density of gas in Fig. 5 and the estimates of the mean star formation rate to calculate the depletion time for the gas in the Universe as a whole. We have used equation (15) in Madau & Dickinson (2014) to estimate the mean star formation rate at each redshift. Fig. 6 shows our estimates of the depletion times for both the CO-traced gas and the dust-traced gas. The dashed line shows the relationship between depletion time and redshift derived for galaxies on the star-forming main sequence and with $\log_{10}(M_*) = 10.5$ (Tacconi et al. 2020), which makes it comparable to the galaxies in our sample. The relationship for the dust-traced gas and that derived from observations of individual galaxies show very similar declines with redshift, although there is an offset as there was for Fig. 5. As with the previous figure, much of the discrepancy might be explained if the temperature of the dust is lower than we have assumed.

5 CONCLUDING REMARKS

We have estimated how the mean density of dust in the Universe varies with redshift using a submillimetre method that has been designed to minimize the effect of dust temperature. We have used the H-ATLAS survey to show that the median temperature of dust in galaxies is $\simeq 22$ K and does not vary with redshift out to $z = 1$. We have then used this temperature and an 850-μm survey of the COSMOS field to estimate the mean density of dust in 10 redshift bins over the range $0 < z < 5.5$. The main uncertainty is whether the dust temperature changes at $z > 1$, although we have argued that both simulations and observations suggest that the mean mass-weighted dust temperature does not vary much with redshift. It will be possible to do a little better in the future using surveys selected at > 1 mm, where the relationship between continuum emission and dust temperature is even weaker, although it will never be possible to remove the bias towards higher temperatures completely.

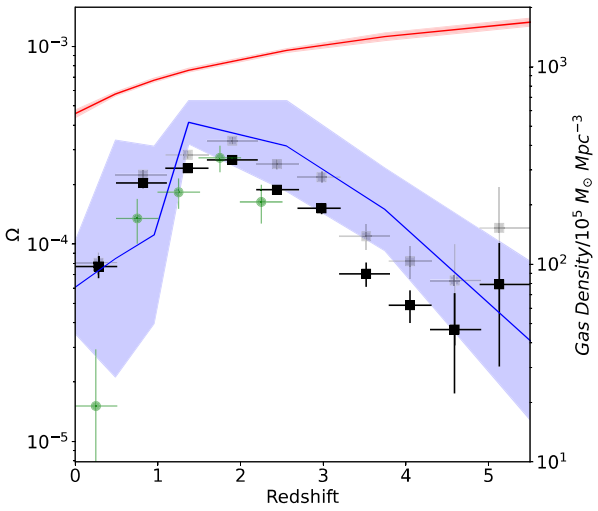

Figure 5. Mean density of hydrogen plotted against redshift, expressed as a fraction of the Universe's critical density on the left-hand axis and as a direct density on the right-hand axis. The black squares are our estimates using the relationship between hydrogen mass and submillimetre luminosity (equation 7). The coloured lines and bands show the best current estimates, and their uncertainties, of the mean density of atomic hydrogen (red) and of the molecular hydrogen traced by CO (blue) (Péroux & Howk 2020). The grey squares are our estimates if we repeat our analysis with a dust temperature of 18 K rather than 22 K. The green symbols show estimates from another study that used the continuum emission from the dust to trace the gas (Garratt et al. 2021).

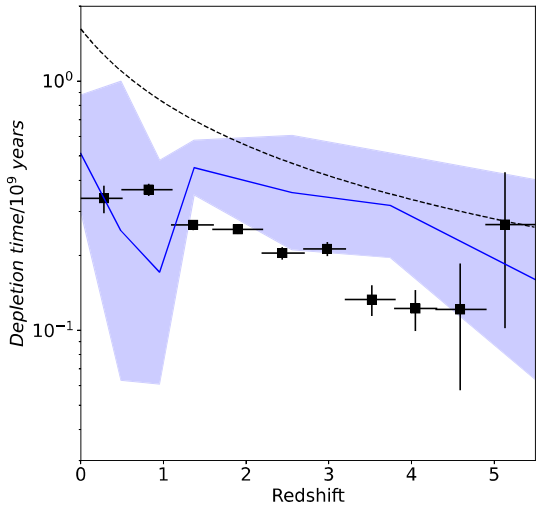

Figure 6. Depletion time versus redshift. The black squares show the estimates for the dust-traced gas. The blue line and band show the estimates and their uncertainty for the CO-traced gas (Péroux & Howk 2020). The dashed line shows an estimate for individual galaxies on the star-forming main sequence and with $\log_{10}(M_*) = 10.5$ (Tacconi et al. 2020).

We find that the mean density of dust in the Universe increased by a factor of $\simeq$10 from $z = 5$ to $z = 2$. It then declined slightly to $z = 1$, and then declined steeply to the present day. The relationship we find is quite similar to the star formation history of the Universe (Fig. 4), although the increase in mean dust density from $z = 5$ to $z = 2$ is steeper than the increase in the star formation rate over the same redshift range. We have also used the submillimetre measurements to estimate the mean density of hydrogen over the same redshift range. We have compared our estimates with estimates in the literature of the mean density of atomic hydrogen and of CO-traced molecular hydrogen. The relationship for atomic hydrogen has a much larger amplitude and a very different redshift dependence than the relationship for our estimates of the gas density. However, the relationship with redshift of our estimates of the gas density (the dust-traced gas) is very similar to the redshift relationship estimated from CO (the CO-traced gas), which implies that most of the dust in the Universe is found in the molecular rather than the atomic phase.

We find that the depletion time for the dust-traced gas in the Universe as a whole declines with redshift in the same way that is seen in the galaxy population (Tacconi et al. 2020).

ACKNOWLEDGEMENTS

This analysis was started while SE was at the conference 'New Views on Feedback and the Baryon Cycle in Galaxies' in Healesville, Australia, in Summer 2023 and continued during a visit to Swinburne University. He thanks the organizers of the conference and the people who made the visit possible. He thanks the Science and Technology Facilities Council (consolidated grant ST/K000926/1) and the Taith fund, Wales' international exchange programme, for the funds for this visit. BW thanks the Science and Technology Facilities Council for a PhD studentship. We thank the referee Matthieu Béthermin for useful comments.

DATA AVAILABILITY

The data from the H-ATLAS, which is used in Section 2.1, are publicly available (h-atlas.org). The data for the COSMOS survey were taken from two papers (Davidzon et al. 2017; Millard et al. 2020).

REFERENCES

Barger A. J., Cowie L. L., Blair A. H., Jones L. H., 2022, ApJ, 934, 56
Bendo G. J. et al., 2023, MNRAS, 522, 2995
Béthermin M. et al., 2015, A&A, 573, A113
Bolatto A. D., Wolfire M., Leroy A. K., 2013, ARA&A, 51, 207
Bourne N. et al., 2016, MNRAS, 462, 1714
Cortese L. et al., 2014, MNRAS, 440, 942
da Cunha E., Charlot S., Elbaz D., 2008, MNRAS, 388, 1595
da Cunha E. et al., 2013, ApJ, 766, 13
Davidzon I. et al., 2017, A&A, 605, A70
Decarli R. et al., 2016, ApJ, 833, 69
Decarli R. et al., 2019, ApJ, 882, 138
Drew P. M., Casey C. M., 2022, ApJ, 930, 142
Driver S. P. et al., 2018, MNRAS, 475, 2891
Dudzevičiūtė U. et al., 2020, MNRAS, 494, 3828
Dunne L., Eales S., Edmunds M., Ivison R., Alexander P., Clements D. L., 2000, MNRAS, 315, 115
Dunne L. et al., 2011, MNRAS, 417, 1510
Dunne L., Maddox S. J., Papadopoulos P. P., Ivison R. J., Gomez H. L., 2022, MNRAS, 517, 962
Dye S. et al., 2010, A&A, 518, L10
Eales S. A., Wynn-Williams C. G., Duncan W. D., 1989, ApJ, 339, 859
Eales S. et al., 2010, PASP, 122, 499
Eales S. et al., 2012, ApJ, 761, 168
Eales S. et al., 2018, MNRAS, 473, 3507
Furlanetto C. et al., 2018, MNRAS, 476, 961
Garratt T. K. et al., 2021, ApJ, 912, 62
Ismail D. et al., 2023, A&A, 678, 271
James A., Dunne L., Eales S., Edmunds M. G., 2002, MNRAS, 335, 753

Liang L. et al., 2019, MNRAS, 489, 1397
Lim C.-F. et al., 2020, ApJ, 889, 80
Madau P., Dickinson M., 2014, ARA&A, 52, 415
Maddox S. J. et al., 2018, ApJS, 236, 30
Magnelli B. et al., 2014, A&A, 561, A86
Ménard B., Fukugita M., 2012, ApJ, 754, 116
Ménard B., Scranton R., Fukugita M., Richards G., 2010, MNRAS, 405, 1025
Millard J. S. et al., 2020, MNRAS, 494, 293
Millard J. S., Diemer B., Eales S. A., Gomez H. L., Beeston R., Smith M. W. L., 2021, MNRAS, 500, 871
Péroux C., Howk J. C., 2020, ARA&A, 58, 363
Planck Collaboration XXII, 2015, A&A, 576, A107
Pozzi F., Calura F., Zamorani G., Delvecchio I., Gruppioni C., Santini P., 2020, MNRAS, 491, 5073
Rémy-Ruyer A. et al., 2014, A&A, 563, A31
Riechers D. A. et al., 2019, ApJ, 872, 7
Schreiber C., Elbaz D., Pannella M., Ciesla L., Wang T., Franco M., 2018, A&A, 609, A30
Scoville N. et al., 2014, ApJ, 783, 84
Simpson J. M. et al., 2017, ApJ, 839, 58
Smith M. W. L. et al., 2010, A&A, 518, L51
Smith M. W. L. et al., 2012, ApJ, 756, 40
Smith M. W. L. et al., 2017, ApJS, 233, 26
Tacconi L. J., Genzel R., Sternberg A., 2020, ARA&A, 58, 157
Valiante E. et al., 2016, MNRAS, 462, 3146
Vlahakis C., Dunne L., Eales S., 2005, MNRAS, 364, 1253
Walter F. et al., 2014, ApJ, 782, 79
Ward B. A. et al., 2022, MNRAS, 510, 2261
Witstok J., Jones G. C., Maiolino R., Smit R., Schneider R., 2023, MNRAS, 523, 3119
Zavala J. A. et al., 2018, MNRAS, 475, 5585

This paper has been typeset from a TEX/LATEX file prepared by the author.